parameter Λ_w. It is noted here that for the time being there are no available experimental data with which to compare for the case of suction and δ/h values larger than $\frac{1}{2}$. When such data becomes available it will be possible to adjust some of the characteristic parameters of the problem if needed.

The present method suggests a closed form approximate solution for a rather complex problem, which was demonstrated to give satisfactory agreement with experiments for the case of no mass transfer, and is expected to predict the effect of mass transfer in the case of suction. This method further indicates the parameters that govern the problem namely, the wall temperature ratio Λ_w, the ratio δ/h, the Mach number M_1, the Reynolds number $Re_{\delta 1}$ and the mass transfer rate $\dot{m}$. Note that the parameter $Re_{\delta 1}$ is proportional to $L/h \cdot h/\delta$, where L the distance from the leading edge to separation and therefore L/h could replace $Re_{\delta 1}$. It appears that $Re_{\delta 1}$ should be the appropriate parameter for design purposes where the local conditions and the boundary-layer thickness are known while L/h should be used to compare with experimental data since in the latter case L/h is usually kept constant.

References

[1] Jakubowski, A. K., Kirchner, R. D., Brown, R. D., and Lewis, C. H., "Experimental Investigation of Heat Transfer and Pressure Distribution in Laminar Separated Flows Downstream of a Rearward Facing Step: Part I No Suction," Engineering Report, Virginia Polytechnic Inst., Blacksburg, Va.

[2] Telionis, D. P. and Swean, T. F., "Approximate Methods for the Calculation of the Heat Transfer Behind a Rearward Facing Step with a Suction Slot," Engineering Report, Virginia Polytechnic Inst., Blacksburg, Va.

[3] Cohen, C. B. and Reshotko, E., "Similar Solution for the Compressible Laminar Boundary Layer with Heat Transfer and Pressure Gradient," Rept. 1293, 1950, NACA.

[4] Weiss, R., "The Near Wake of a Wedge," Research Rept. 197, 1964, Avco Everett Research Lab., Everett, Mass.

[5] Su, W. M. and Wu, J. M., "Base Pressure Correlation in Supersonic Flow," *AIAA Journal*, Vol. 9, No. 7, July 1970, pp. 251–255.

[6] Rom, J. and Seiginer, A., "Laminar Heat Transfer to a Two-Dimensional Backward Facing Step from the High Enthalpy Flow in the Shock Tube," *AIAA Journal*, Vol. 2, No. 2, Feb. 1964, pp. 251–255.

[7] Holloway, P. F., Sterett, J. R., and Creekmore, H. S., "An Investigation of Heat Transfer within Regions of Separated Flow at a Mach Number of 6.0," TN D-3074, 1965, NASA.

† Note that in the present notation y is defined as the ordinate of a streamline before expansion, it is therefore introduced here a modified stream function.

‡ Note added in proof: Dr. Jakubowski has recently informed the author that some initial experimental result indicate that q_r/q_s might be a little overestimated in Fig. 3. Yet the inability to measure accurately the mass transfer rate and the small number of experimental points would not permit a comparison.

Particle Charging behind Shock Waves in Suspensions

B. M. SHIRLEY* AND J. W. SHELDON†
Florida State University, Tallahassee, Fla.
AND
S. C. KRANC
University of South Florida, Tampa, Fla.

Received February 8, 1972; revision received March 20, 1972. Research supported in part by NSF Grant GK 5343.

Index category: Multiphase Flows.

* Research Assistant.

† Associate Professor, School of Engineering Science.

Assistant Professor, Department of Structures, Materials, and Fluids. Associate Member AIAA.

Nomenclature

J = particle flux
L = velocity equilibration length
r = radius
R = rate of collision
U = particle velocity
v = gas velocity
X = distance behind shock

Subscripts

d = downstream
i = particle class index
m = maximum
u = upstream
μ = viscosity
ρ = density

DURING an experimental investigation of shock structure in gases containing dust suspensions, substantial electrical signals associated with the shock wave were observed. A series of qualitative experiments was conducted to determine the mechanism producing these signals.

These experiments were conducted in an ordinary pressure driven shock tube made of aluminum tubing 5.7 cm in diameter and operated in a vertical position. A measured mass of glass particles supplied by Heat Systems-Ultrasonics and having a nominal size distribution of 5μ diameter was introduced into the test section while a gentle gas flow from below was maintained to keep the suspension uniform. Maximum densities obtained in this manner were approximately 10^7 particles/cm^3, calculated by assuming an even distribution of particles in the test section. The tube was instrumented with a piezoelectric pressure transducer and an electrical probe at an observation station located 71 cm from the diaphragm. The probe consisted of a short length of bare wire aligned in the flow by a grounded shield. The voltage from probe to ground and the pressure trace were recorded simultaneously on a dual channel oscilliscope.

In the first experiment, a relatively weak shock ($M = 1.15$) was propagated in the test section. The oscilliscope traces presented in Fig. 1a demonstrate the development of a voltage signal behind the shock wave as it passes through the suspension. Two different loadings are shown. Similar signals were observed for other particulate matter such as ammonium chloride and tin oxide. In a second experiment, a rarefaction wave was propagated in the test section through the suspension by evacuating the chamber on the other side of the diaphragm until rupture occurred. Figure 1b shows the pressure and voltage traces during the passage of a rarefaction wave. No signals were observed when particles were not present in the test section during the passage of a wave.

We considered several possible causes for these signals. While the particles were not intentionally given an initial charge, all dusts do have some residual charge but this is generally quite small. Particle collisions with the probe are ruled out since

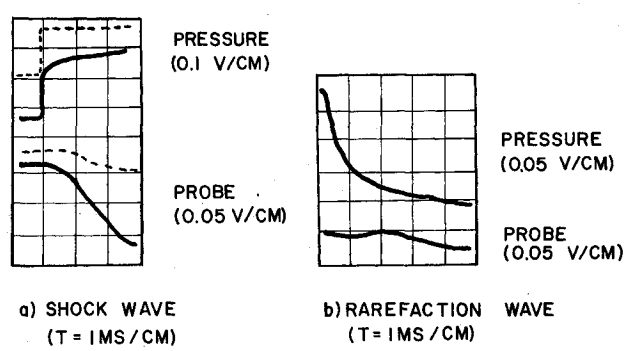

Fig. 1 Comparison of electrical signals for a) shock wave and b) rarefaction wave. Velocities behind waves are approximately 80 m/sec and 276 m/sec, respectively. Particle loading effects decrease actual velocities and degrade pressure traces as shown. (Solid lines indicate particle loading 10^7/cm^3, dotted line indicates 5×10^6/cm^3.)

signals can be obtained by substituting a glass test section and placing the probe outside. Interactions between the particles and the wall resulting in particle charging are difficult to rule out completely even though the metal wall was grounded.[1] However, this mechanism does not appear to be consistent with the results for the rarefaction wave since only a weak electrical signal was observed for this wave even though the velocity developed behind the wave is considerably greater than that behind the shock wave. We conclude that particles are charged by collisions in the flow behind the shock wave.

The mechanism for charging by interparticle collision may be discussed in terms of the following heuristic model. As explained by others,[2] particles of different sizes develop velocity lags behind the shock wave. If we use Stokes' drag law to estimate the aerodynamic force on a particle with radius r_i, then the particle's velocity U_i a distance X downstream of the shock is given approximately by

$$U_i = v_d + (v_u - v_d)\exp(-X/L_i) \quad (1)$$

when $|v_u - v_d| \ll v_d$. The upstream and downstream gas velocities are given by v_u and v_d, respectively, and L_i is the velocity equilibration length given by Marble[2] in the form

$$L_i = 2\rho v_d r_i^2/9\mu \quad (2)$$

where ρ is the density of particle material and μ is the gas viscosity. The maximum relative velocity between particles with radii r_1 and r_2 then occurs at a distance X_m downstream of the shock. X_m may be obtained from Eq. (1)

$$X_m = \frac{2\rho v_d r_1^2 r_2^2 \ln(r_1/r_2)}{9\mu(r_1^2 - r_2^2)} \quad (3)$$

Estimation of R, the rate of collisions per unit volume, for a simple single collision model yields

$$R = J_1 J_2 \pi (r_1 + r_2)^2 |(U_1 - U_2)/U_1 U_2| \quad (4)$$

where J_i is the ith particle flux. Thus, to the same order of approximation used above, the maximum collision rate occurs at X_m.

Collision can cause initially neutral particles to become charged as discussed by Kunkel[3] and an electric field would be produced as they separate after encounter. Since the maximum collision rate occurs downstream of the shock rather than at the discontinuity, the electric field would increase gradually as we have observed in these experiments. The same mechanism can occur in the case of the rarefaction wave but because of the decrease in particle density the resultant signals should be of a much smaller magnitude.

Temkin[4] has also examined particle collision in a comparable experiment. A suspension of droplets was subjected to repeated shock waves and droplet agglomeration as a result of collision was observed. A principal mechanical effect of collisions is to bring about momentum exchange between particles of different sizes as pointed out by Marble.[3] The importance of these works as well as the present study is to indicate some of the possible effects of interparticle collisions which have not been generally included in theoretical treatments of shock structure in particle suspensions.[5]

References

[1] Torobin, L. B. and Gauvin, W. H., "Fundamental Aspects of Solids-Gas Flow Part VI: Multiparticle Behavior in Turbulent Fluids," *The Canadian Journal of Chemical Engineering*, Vol. 39, No. 6, June 1961, pp. 113–120.

[2] Marble, F. E., "Mechanism of Particle Collision in the One Dimensional Dynamics of Gas Particle Mixtures," *The Physics of Fluids*, Vol. 7, No. 8, Aug. 1964, pp. 1270–1282.

[3] Kunkel, W. B., "The Static Electrification of Dust Particles on Dispersion into a Cloud," *Journal of Applied Physics*, Vol. 21, No. 8, Aug. 1950, pp. 820–832.

[4] Temkin, S., "Droplet Agglomeration Induced by Weak Shock Waves," *The Physics of Fluids*, Vol. 13, No. 6, June 1970, pp. 1639–1641.

[5] Kriebel, A. R., "Analysis of Normal Shock Waves in a Particle Laden Gas," *Transactions of the ASME, Ser. D: Journal of Basic Engineering*, Vol. 86, 1964, pp. 655–665.

Prediction of Nose Shape Effects on Nonlinear Stability Characteristics of Slender Cones

LARS E. ERICSSON* AND ROLF A. GUENTHER†
Lockheed Missiles & Space Company, Sunnyvale, Calif.

Nomenclature

C_{DN} = nose drag coefficient, $C_{DN} = D_N/(\rho U^2/2)(\pi d_N^2/4)$
C_m = pitching moment coefficient $C_m = M_p/(\rho U^2/2)(\pi d_B^3/4)$
d_B = base diameter
d_N = nose bluntness diameter
l = sharp cone length
q = rigid body pitch rate, $\dot{\alpha} = q$
U = velocity
x = axial body coordinate
$\Delta\bar{x}$ = cone center of gravity location forward of base
$\Delta\bar{x}_{CP}$ = cone center of pressure location forward of base
θ_c = cone frustum half-angle
θ_N = half-angle of conical tip
$\kappa_N, \bar{\kappa}_N$ = hypersonic scaling parameters for nose directing effects, defined in Eqs. (2) and (4)
ρ = air density
$\chi_l, \bar{\chi}_l$ = hypersonic scaling parameters for nosee drag effects, defined in Eqs. (1) and (3)
$C_{m\alpha}$ = static stability derivative, $C_{m\alpha} = \partial C_m/\partial\alpha$
$C_{mq} + C_{m\dot{\alpha}}$ = dynamice stability derivative, $C_{mq} + C_{m\dot{\alpha}} = \partial C_m/\partial(d_B\dot{\alpha}/U) + \partial C_m/\partial(d_B q/U)$

IT has been well domcumented that nose bluntness has a large effect on slender cone vehicle dynamics.[1-5] Only spherical nose bluntness has in general been investigated. Recently it has been shown that a change of nose shape from spherical to conical can change the vehicle characteristics substantially.[6,7] The conical nose tip geometry approximates the expected vehicle

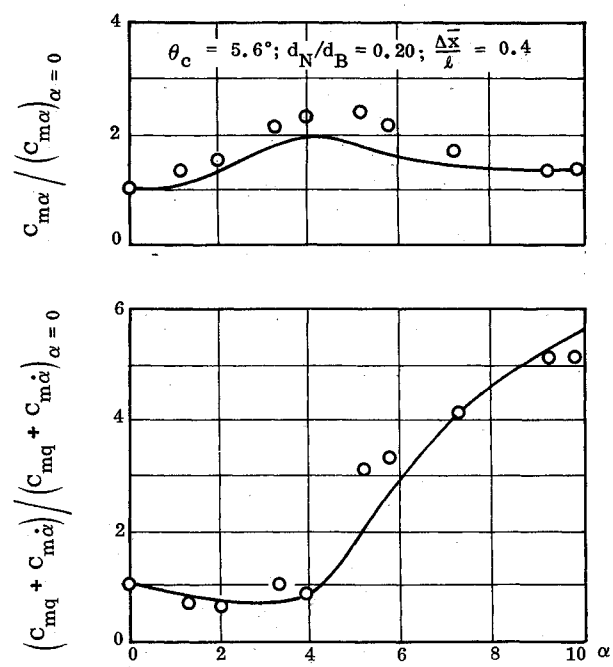

Fig. 1 Effect of angle of attack on the stability characteristics of a 20% blunt 5.6° cone with spherical nose bluntness.

Received February 9, 1972.
Index categories: Entry Vehicle Dynamics and Control; Nonsteady Aerodynamics; Supersonic and Hypersonic Flow.

* Senior Staff Engineer. Associate Fellow AIAA.
† Senior Aerodynamics Engineer.